MECSOL 2022 - Proceedings of the 8th International Symposium on Solid Mechanics
M.L. Bittencourt, J. Labaki, L.C.M. Vieira Jr. and E. Mesquita (Editors), Campinas SP, Brazil, October 17th to 19th, 2022

Fatigue and residual stresses – a deleterious combination

Danielle Lopes Zaidan[1], Yan Cavalcante Buarque[1], Paulo Pedro Kenedi [1,2], Luís Felipe Guimarães de Souza[1,2]

[1] Programa de Pós-graduação em Engenharia Mecânica e Tecnologia de Materiais - PPEMM - CEFET/RJ; Av. Maracanã, 229 - RJ - Brazil.

[2] Curso de Engenharia Mecânica - CCGMEC-CEFET/RJ; Av. Maracanã, 229 – RJ - Brazil.

Abstract: *Mechanical parts submitted to loads that partially yields its transversal cross sections, generates residual stress distributions, which can produce deleterious effects. An analytical model is proposed, using Mechanics of Solids, merging residual stress and fatigue analytical approaches, to estimate the specimen's fatigue lives. Curvatures are imposed on steel flat bars specimen to partial yield its cross sections. After the spring back, the curved specimens, with different residual stress distributions, are submitted to a bending fatigue load. The proposed analytical model quantifies how deleterious the residual stress can be for the analysed specimens.*

Keywords: residual stress, analytical model, fatigue

INTRODUCTION

Residual stress is a wide matter, which is usually accessed by experimental approaches. The analytical approaches tend to be scarce, except by the simple ones, as in Crandall *et al*. (1988). In fact, the analytical approaches have some limitations related, for instance, to cross sections and loadings. Nevertheless, the analytical approaches can estimate the residual stress cross section distribution, not only the residual stress at the surfaces, as is the case of well-established experimental techniques, Schajer (2013). Castro and Meggiolaro (2009) and Jirásek (2002) are interesting references for residual stress analytical models; as well in Stok (2008). Also, Castro *et al*. (2020), Castro *et al*. (2019), Zaidan *et al*. (2019), Castro (2018), Vargas (2014) and Lopes (2013) have examples of application of the analytical approach models to estimate the residual stress distribution of partially yielded structures of rectangular cross sections. Still, Riagusoff *et al*. (2010) utilized a hollow circular cross section in their analytical formulation, and Vignoli and Kenedi (2019) accessed the residual stress distribution in composite beams.

In this work, it is proposed an analytical model to describe the adverse effect of residual stresses in the fatigue life of partially yielded structures. To achieve this objective, it is proposed submit specimens, with pre-existing residual stress distributions, to a fatigue loading. The proposed analytical model is divided in two phases. Phase 1, it is characterized by the application of a monotonic transversal load, by a former, on flat bar specimens, through the utilization of a three-point bending apparatus, as shown in Fig. 1.a. The transversal load must be sufficient to partially yield the specimens cross sections. After the spring back, a residual stress distribution pattern is generated in its cross sections. In sequence, in the phase 2, it is applied a variable transversal loading on the specimens, using the same three-point bending apparatus, until one of the two results happens: a crack is generated in the specimen and ultimately breaks, or the specimen has infinite life and endure for more than a certain number of cycles (typically 10^6 cycles).

Note that in the phase 1, the same cross-section residual stress distribution was produced in all flat bar specimens' cross sections, with compressive residual stress at extrados (point *a*) and tensile residual stress at intrados (point *b*), as shown in Fig.1.a. At phase 2 the positive curvature specimens (PCS) will sense a tensile fatigue load at point *a*, while the negative curvature specimens (NCS) will sense a tensile fatigue load at point *b*, both on a three-point bending apparatus, as shown, respectively, in Fig. 1.b and Fig. 1.c. Specimens without any curvature (residual stress free) are also used, to serve as reference.

Fig.1 show the schematic draw of the loading phases: phase 1, consisting in a monotonic loading, to generate the residual stress distributions and phase 2, consisting in the application of the fatigue loading.

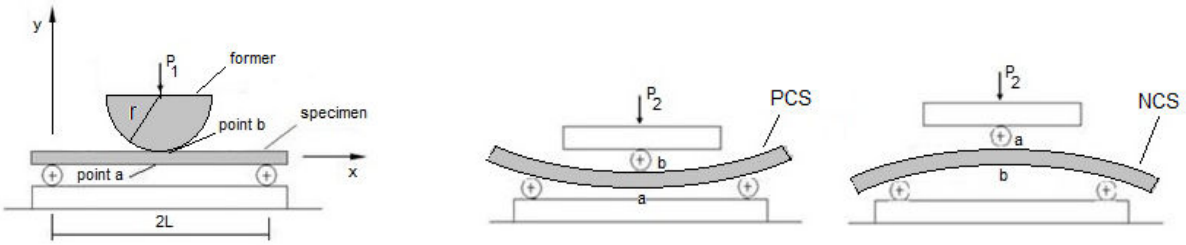

(a) (b) (c)

Figure 1. (a) Phase 1, monotonic loading with P_1. Phase 2, Fatigue loading with P_2: (b) positive curvature specimen (PCS) and (c) negative curvature specimen (NCS).

Where 2L is the length of specimens between the rollers. The positive curvature, the straight specimen and the negative curvature are abbreviated, respectively, as PCS, RSFS and NCS.

DEVELOPMENT

In this section the formulation of the proposed analytical model is explained, defining the hypothesis, limitations, and advantages of these two phases approach.

Analytical model

The analytical model is based in mechanics of solids, as in Crandall *et al*. (1988). It is used to estimate the residual stress effect in the life of specimens submitted to variable loading. It is supposed that prior to the phase 1, that the specimens are residual stress-free. For the phase 1 a transversal load increases monotonically until the specimen embrace the former, at P_1 load. After the removal of P_1, followed by spring back, a cross-section residual stress distribution is generated. For the phase 2 the transversal load P_2 is applied in a sinusoidal pattern, generating an elastic cross-section stress distribution, that are summed up to the existent residual cross section stress distribution.

In the phase 1, the specimens are loaded by an imposed monotonic transversal force P_1, through the utilization of a semi-circular former of *r* radius. The beginning of yield moment M_y, the fully plastic moment M_p and the imposed bending moment $M_1(\rho_1)$, can be estimated, for a bi-linear strain-hardening material, as in Crandall *et al*. (1988):

$$M_y = \frac{2}{3} b c^2 S_y \qquad \rho_y = \frac{E}{S_y} \cdot c \qquad \rho_1 = r + c \tag{1}$$

$$M_1(\rho_1) = \frac{3}{2} \cdot \left[1 + \frac{1}{3} \cdot \left(-1 + \frac{E_t}{E} \right) \cdot \left(\frac{\rho_1}{\rho_y} \right)^2 + \left(\frac{2}{3} \cdot \left(\frac{\rho_1}{\rho_y} \right)^{-1} - 1 \right) \cdot \frac{E_t}{E} \right] \cdot M_y \qquad P_1(\rho_1) = \frac{2}{L} \cdot M_1(\rho_1) \tag{2}$$

$$M_p = \frac{3}{2} \cdot \left[1 + \left(\frac{2}{3} \cdot \left(\frac{\varepsilon_u}{\varepsilon_y} \right) - 1 \right) \cdot \frac{E_t}{E} \right] \cdot M_y \tag{3}$$

Where, *b* and *c* are, respectively, the width and the semi-height of the specimen cross-section. S_y is the yield strength, *E* and E_t are, respectively, the Young and the tangent modulus. ρ_1 and ρ_y are, respectively, the imposed radius of curvature and the initial yielding radius of curvature. ε_y and ε_u are, respectively, the yield and the ultimate strains. Fig. 2 shows the specimen rectangular cross-section partially yielded, where y_y is the elastic-plastic border.

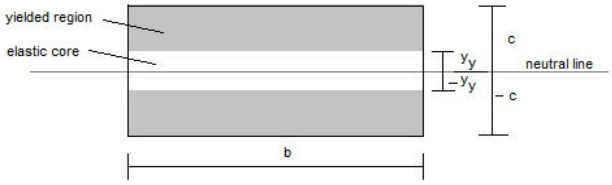

Figure 2. Specimen partially yielded cross-section.

The cross-section stress distributions equations for loading σ(y), unloading (spring back) $\sigma_{sb}(y)$ and residual stress $\sigma_{res}(y)$ are shown by equations (4-7):

$$\sigma(y) = \begin{cases} -S_y - E_t \cdot \left(\frac{y}{\rho_1} - \varepsilon_y\right) & for\ y_y < y \leq c \\ \frac{y}{y_y} \cdot S_y & for\ -y_y < y \leq y_y \\ S_y - E_t \cdot \left(\frac{y}{\rho_1} + \varepsilon_y\right) & for\ -c < y \leq -y_y \end{cases} \tag{4}$$

$$E_t = \frac{S_{ut} - S_y}{\varepsilon_u - \varepsilon_y} \qquad y_y = c \cdot \sqrt{3 - 2 \cdot \frac{M_1(\rho_1)}{M_y}} \tag{5}$$

$$\sigma_{sb}(y) = \frac{M_1(\rho_1) \cdot y}{I} \qquad I = \frac{b \cdot (2 \cdot c)^3}{12} \tag{6}$$

$$\sigma_{res}(y) = \sigma(y) + \sigma_{sb}(y) \tag{7}$$

Where *I* is the second moment of area and *y* is a vertical position in the specimen cross-section (it is zero at neutral line) and S_{ut} is the ultimate strength. Fig.3 shows the lateral view of the residual stress generation sequence of phase 1. Fig.3.a shows the cross-section stress distribution for P_1 loading, Fig. 3.b shows the spring back stress distribution after the P_1 removal and Fig. 3.c shows the resultant cross-section residual stress distribution. Note that cross-section residual stress distribution generation for both PCS and NCS, at phase 1, are almost the same. The residual stress distribution difference arises by the curvature that the specimen is used on the three-point bending apparatus in phase 2. For the PCS, the residual stress distribution maintains the same shown in the Fig.3.c, whereas for the NCS, the residual stress distribution shown in the Fig.3.c must be multiplied by -1.

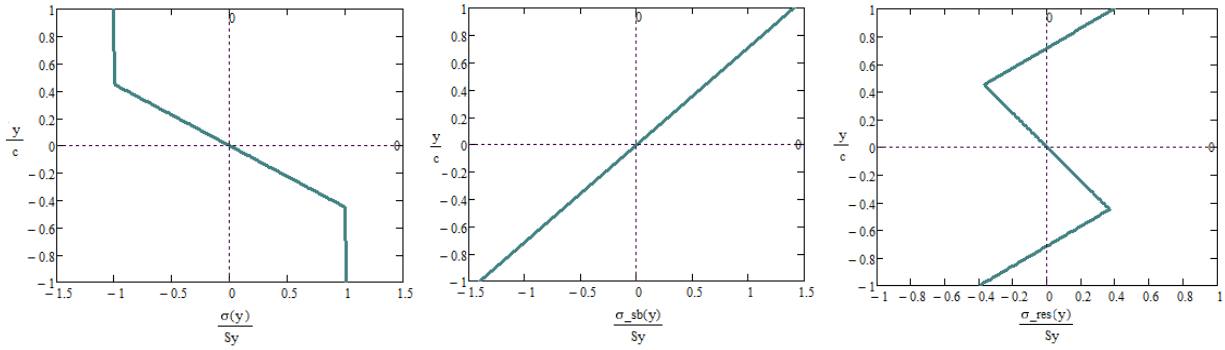

(a) (b) (c)

Figure 3. Cross-section stresses generation sequence (lateral view): (a) loading, (b) unloading (spring back) and (c) residual stress distribution.

Note that the radius of curvature ρ_1, show in equation (1.c), was select to keep the imposed bending moment $M_1(\rho_1)$ in an intermediary value, as shown in Table 1. In the phase 2, a sinusoidal fluctuating elastic loading is imposed:

$$\sigma_{x_{max}} = \sigma_{res} + \beta \cdot S_y \qquad \sigma_{x_{min}} = \sigma_{res} + R \cdot \beta \cdot S_y \qquad \sigma_{x_m} = \frac{\sigma_{x_{max}} + \sigma_{x_{min}}}{2} \qquad \sigma_{x_a} = \left|\frac{\sigma_{x_{max}} - \sigma_{x_{min}}}{2}\right| \tag{8}$$

Where σ_{res} is the residual stress result, of a cross section selected point *y*, β is a positive multiplier, smaller than 1. The β is chosen to turn $\sigma_{x_{max}}$ of NSC equal to a high elastic stress. *R* is the stress ratio between $\sigma_{x_{min}}$ and $\sigma_{x_{max}}$ which are, respectively, the minimum and the maximum stresses. σ_{x_m} and σ_{x_a} are, respectively the mean and the alternating stresses, for a cross section select point. Later on, it will be explained which cross section select point will be utilized, the y = - c or the y = - y_y.

Fig. 4 shows the three different loading sequences for PCS, RSFS and NCS, for phases 1 and 2, for a cross section critical point y = -c.

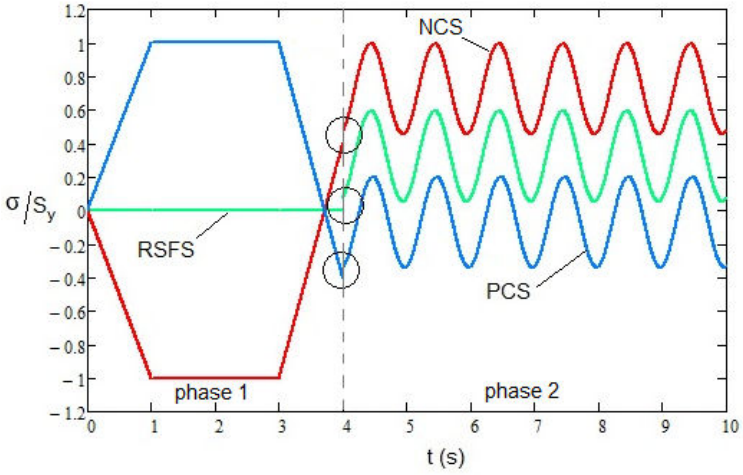

Figure 4. Loading sequences, in a stress vs time graphic, for phases 1 and 2, at y = -c.

The sinusoidal loading values of phase 2, which are available in Table 2, occurs until the specimen breaks (finite life) or the test is stopped, after a certain number of cycles (for instance, 10^6 cycles), that characterizes infinite life. Note, that in Fig. 4, there are discontinuities between the end of phase 1 and the beginning of phase 2, marked with black circles. This happens because phase 2 starts with a minimum stress. This is a practical imposition, to maintain the specimen always submitted to some external load. The vertical axis of Fig. 4 is in scale, while the horizontal is not. For instance, the sinusoidal loadings frequency appears to be around 1 Hz, but can be set, evidently, to a higher frequency.

An interesting effect arise, in Fig. 4, when the same sinusoidal stress range (σ_{max} - σ_{min}) is applied for all the three cases. In phase 2, the NCS sinusoidal curve is shifted to the upper part of Fig. 4, by summing the tensile residual stress of phase 1 with the tensile sinusoidal loading of phase 2, producing a combined loading (phase 1 + phase 2) with a huge σ_{x_m}, as shown in Table 2.

To implement the classical fatigue model in phase 2, the fatigue limit S_e must be accessed, as in Budynas and Nisbett (2016).

$$S_e = 4.51 \cdot (S_{ut})^{-0.256} \cdot \left[\frac{0.808 \cdot \sqrt{b \cdot h}}{7.62}\right]^{-0.107} \cdot 1 \cdot 1 \cdot 1 \cdot 1 \cdot 0.5 \cdot S_{ut} \tag{9}$$

Where, $h = 2 \cdot c$ is the height, in mm, of the specimen cross-section. The modified Goodman curve is used as fatigue failure criterium. So, the following equations are used:

$$\sigma_m = \sqrt{{\sigma_{x_m}}^2 + 3 \cdot {\tau_{xy_m}}^2} \qquad \sigma_a = \sqrt{{\sigma_{x_a}}^2 + 3 \cdot {\tau_{xy_a}}^2} \qquad A = \frac{\sigma_a}{\sigma_m} \tag{10}$$

$$n = \left[\frac{\sigma_a}{S_e} + \frac{\sigma_m}{S_{ut}}\right]^{-1} \tag{11}$$

Where A is the slope of the load line, σ_m and σ_a, are, respectively, the mean and the alternating von Mises equivalent stresses and n is the fatigue factor of safety. The values of σ_{x_m} and σ_{x_a} are estimated by equation (8). It is considered that the shear stresses, imposed by the variable transversal load P_2, was not significant. Also, there is no torsion loading, so τ_{xy_m} and τ_{xy_a} are considered null. If $n > 1$, it is established that the specimen has infinite life, otherwise the number of cycles of the finite life N can be estimated by the equation (12).

$$\sigma_{a\_eq} = \left(1 - \frac{\sigma_m}{S_{ut}}\right)^{-1} \cdot \sigma_a \qquad N = \left(\frac{\sigma_{a\_eq}}{a}\right)^{\frac{1}{b}} \qquad a = \frac{(f \cdot S_{ut})^2}{S_e} \qquad b = -\frac{1}{3} log\left(\frac{f \cdot S_{ut}}{S_e}\right) \tag{12}$$

Note that the alternating equivalent stresses σ_{a_eq} of equation (12.a) was used to adjust the actual loading (that has mean and alternating parcels) to being used in the equation (12.b), that was formulated for completely alternating load.

Model implementation

The Mathcad software was used to implement the calculus and generate graphical results of the proposed analytical model. The calculus development used equations (1-12) and Tables (1-2) inputs to generate the Table 3 results and Figure (5-7) results. Specimens made of steel flat bars, with inputs of Table 1, were simulated using the proposed analytical model: loaded monotonically in phase 1, to generate the residual stress patterns, and, in sequence, they are submitted in phase 2 to a fatigue loading until having a failure (finite life) or not having a failure (infinite life).

Table 1 – Geometrical / material / loading inputs

Geometrical characteristics					
b (mm)	c (mm)	2L (mm)	ρ_y (m)	ρ_1 (m)	r (mm)
14	3	200	0.571	0.257	254
Loading					
M_y (N·m)	M_1(N·m)	M_p (N·m)	y_y/c	R	β
91.4	128.3	149.3	0.45	0.1	0.6
Material properties					
E (GPa)	E_t (GPa)	S_y (MPa)	S_{ut} (MPa)	ε_y (m/m)	ε_u (m/m)
207	1.2	1088	1237	$5256 \cdot 10^{-6}$	0.128
Other constants					
f (*)	I (m^4)	S_e (MPa)			
0.785	$2.52 \cdot 10^{-10}$	424			

(*) Obtained in Budynas and Nisbett (2016)

Note in Table 1 that $\rho_1 < \rho_y$, $M_y < M_1 < M_p$, so the specimens are partially yielded. Table 2 shows the loading characteristics used in phase 2, for $M_2 = 54.8$ N·m.

Table 2 – Phase 2 loading

	PCS_c	PCS_ y_y	RSFS	NCS
σ_{x_m}/S_y	-0.07	0.16	0.33	0.73
σ_{x_a}/S_y	0.27	0.27	0.27	0.27
$\sigma_{x_{min}}/S_y$	-0.34	-0.11	0.06	0.46
$\sigma_{x_{max}}/S_y$	0.20	0.43	0.6	1.0

Note that σ_{x_a}/S_y are the same for the three types of specimens (PCS, RSFS and NCS), while the σ_{x_m}/S_y are not. Also, there is another constant in phase 2 loadings, the loading range: $(\sigma_{x_{max}}/S_y - \sigma_{x_{min}}/S_y) = 0.54$. See Fig. 5.a to realize the difference between PCS_c and PCS_ y_y.

The Fig.5 shows the final stress cross distribution for the three types of specimens (PCS, RSFS and NCS).

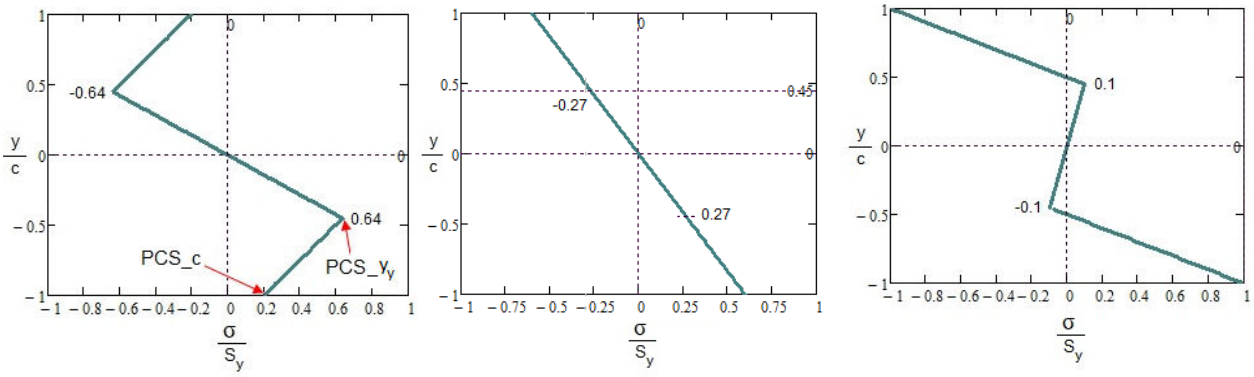

(a) (b) (c)

Figure 5. Final stress specimen cross distribution (lateral view): (a) PCS, (b) RSFS and (c) NCS.

The Fig. 5 graphics shows the sum of the residual stress distribution of phase 1, for instance shown at Fig. 3.c for PCS, and the stress distribution of phase 2. As RSFS is residual stresses free, Fig. 5.b only shows the maximum elastic load distribution of phase 2. Note that the maximum final stresses of RSFS and NCS occurs at y/c = +1 and y/c = -1, but the maximum final stresses of PCS occur at y_y/c = + 0.45 and at y_y/c = - 0.45, named PCS_y_y. In fact, PCS_y_y, with σ/S_y = 0.64, is 3.2 times larger than PCS_c, with σ/S_y = 0.2.

Figure 6 shows another way to represent the loading applied on the three different types of specimens (PCS, RSFS and NCS), in a stress vs strain graphic. The dark gray line represents the phase 1 and the color filled squares/lines represents the phase 2 of loading.

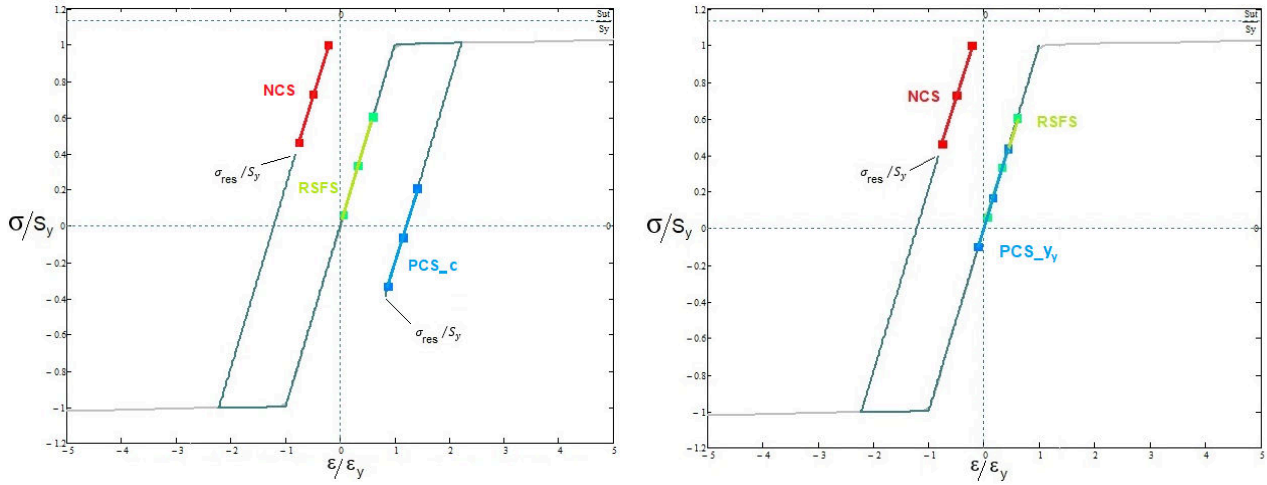

(a) (b)

Figure 6. Stress vs strain graphic. Phase 1: dark gray continuous line. Phase 2: with color lines/square points. (a) PCS_c, RSFS and NCS, all at y = - c and (b) PCS_y_y for y = - y_y and RSFS and NCS for y = - c.

Fig. 6, show, in a quite complete way, what happens with each specimen type (PCS, RSFS and NCS), joining phases 1 and 2 of loading. The NCS, which have tensile stresses in both phases, shows the highest stress results. The RSFS, which not have phase 1, only phase 2, presents an intermediary behavior. The PCS, which is represented in Fig 6.a by PCS_c (at y = -c) and in Fig. 6.b by PCS_y_y (at y = -y_y), shows the lowest stresses of all, because have compressive stresses in phase 1 and tensile stresses in phase 2. Note that PCS_y_y is the real PCS response of the specimen because it represents the cross section critical point. For one hand it is evident that the tensile residual stress has a deleterious effect in NCS. For other hand, the compressive residual stress does not have so substantial "beneficial" effect, considering the PCS_ y_y behavior of Fig. 6.b, where the blue color filled squares/lines of PCS_ y_y are almost in same region of the green color filled squares/lines of RSFS, with no residual stress.

Figure 7 shows an usual fatigue graphic of alternating stress vs mean stress, with results of application of the Modified Goodman criterium for all three types of specimens (PCS, RSFS and NCS).

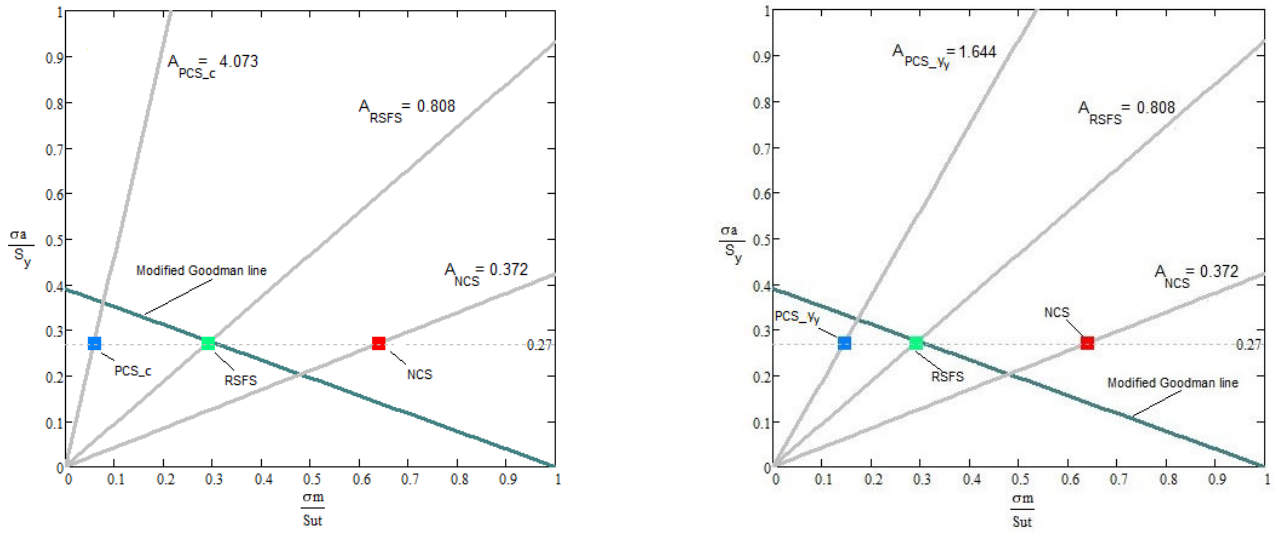

Figure 7. Alternating stress vs mean stress graphics, (a) all specimens with y = - c and (b) PCS_y_y with y = y_y and RSFS and NCS with y = - c.

Fig. 7 show a classical graphical output for fatigue results. The only difference between Fig.7.a and 7.b, is the PCS operation point. Both operation points, represented by a blue square, PCS_c and PCS_y_y, still maintain inside the infinite life region. Note that the PCS_y_y point is dislocated to the right, getting closer to the Modified Goodman line, which divide the infinite and finite life regions. In terms of mechanical design, it can be said that the diagram shows in the Fig.7.b is the "correct" one, as it shows the effect of the maximum combination of σ_a and σ_m of the specimen at its most critical point. In Fig.7.b, the operation point of RSFS and NCS is related to y = -c (specimen bottom), the operation point for the PCS_y_y is related to y = - y_y (elastic-plastic border).

Analyzing Fig. 7, it is clear that PCS and RSFS has infinite life, whilst NCS has a finite life. In Table 3 the results of the fatigue safety factor *n* or of the number of cycles until failure *N* of the specimens, calculated using the Mathcad software, are shown.

Table 3 – Specimens fatigue safety factor *n* (infinite life) or number of cycles for failure *N* (finite life)

	PCS_c	PCS_y_y	RSFS	NCS
n or *N*	1.331	1.194	1.017	4383 cycles

Analyzing the Table 3, it is clear that "beneficial" effect of residual stress in PCS, as have, in the cross section critical point, compressive stresses in phase 1 and tensile stresses in phase 2, that generated a n = 1.194, it was not so much better that the safety factor of 1.017 obtained for RSFS, which was residual stress free. On the other hand, the deleterious effect in NCS, which have, at the cross section critical point, has tensile stresses, for both, residual and fatigue loadings, produced an particularly short finite life.

CONCLUSIONS

The proposed analytical model analyzed the influence of the residual stress distribution in the fatigue life of steel flat bars specimens. To accomplish this objective, in phase 1, different cross section stress distributions are imposed to steel flat bars specimens. In phase 2 the same sinusoidal stress range and alternating stress were applied to the specimens, through the imposition of fatigue loading. The well-established modified Goodman criterium was used to determine the final condition of the specimens: finite or infinite life. The utilization of several graphics as σ vs *t*, *y* vs σ, σ vs ε and

σ_a vs σ_m, served to enhance the understanding of the effect of the cross section residual stresses in the fatigue life of steel flat bars specimens. The specimens submitted with tensile residual stress and tensile fatigue load stress produced a very short finite life, whilst for specimens submitted the same tensile fatigue load stress, but with a compressive residual stress or, even with no residual stress, produced infinite life.

Also, two point deserves to be highlighted. a) Not always the cross section critical point of mechanical parts, with residual stresses induced by bending loading, are located at free surfaces and b) Even when in the critical point exists compressive residual stresses, the "beneficial effects" it might not be much better that if the mechanical part does not have any residual stress at all.

The overall conclusion is that residual stresses do influence, in a deleterious way, the fatigue life of partially yielded mechanical parts. The experimental part of this research is under implementation.

REFERENCES

Budynas, R.G and Nisbett, J.K., 2016, "Elementos de Máquinas de Shigley". McGraw-Hill Education.Brazil.

Castro, F.A., Kenedi, P.P., Vignoli, L.L., Riagusoff, I.I.T, 2020, "Residual stress distribution in built-in beams", Proceedings of the Institution of Mechanical Engineers, Part L: Journal of Materials: Design and Applications, Vol. 235, pp. 216-231. https://doi.org/10.1177/1464420720958617.

Castro, F.A., Kenedi, P.P., Vignoli, L.L. and Riagusoff, I.I.T., 2019, "Residual stress distribution in hyperstatic beams". Proceedings of the VII International Symposium on Solid Mechanics - MECSOL 2019, São Carlos, Brazil. https://doi.org/10.26678/ABCM.MECSOL2019.MSL19-0088.

Castro, F.A., 2018, "Análise de tensões residuais em estruturas hiperestáticas", Master Thesis in portuguese, Centro Federal de Educação Tecnológica Celso Suckow da Fonseca - CEFET/RJ, Rio de Janeiro, Brazil.

Castro, J.T.P., Meggiolaro, M.A., 2009, "Fadiga – Técnicas e Práticas de Dimensionamento Estrutural sob Cargas Reais de Serviço. Volume 1- Iniciação de Trincas", Amazon books.

Crandall, S.H., Dahl, N.C., Lardner,T.J., 1988, "An Introduction to the Mechanics of Solids", Second Edition with SI units, McGraw-Hill International Editions.

Jirásek, M. and Bazant, Z.P., 2002, "Inelastic Analysis of Structures", John Wiley and Sons Ltd.

Lopes, D.G., 2013, "Avaliação das tensões residuais na montagem de conectores em armaduras de tração de dutos flexíveis", Master Thesis in portuguese, Centro Federal de Educação Tecnológica Celso Suckow da Fonseca - CEFET/RJ, Rio de Janeiro, Brazil.

Riagusoff, I.I.T., Kenedi, P.P., Souza, L.F.G., Pacheco, P.M.C.L., 2010, "Modeling of Pipe Cold Bending: A Finite Element Approach", Proceedings of the VI Congresso Nacional de Engenharia Mecânica - CONEM 2010, Campina Grande, Brazil.

Schajer, G.S., 2013, "Practical Residual Stress Measurements Methods". Wiley.

Stok, B., Halilovic, M., 2008, "Analytical solutions inelasto-plastic bending of beams with rectangular cross section", Applied Mathematical Modelling, Vol. 33, pp. 1749-1760.

Vargas, F.A., 2014, "Avaliação das tensões residuais em armaduras de tração de dutos flexíveis pelo método experimental da rede de Bragg", Master Thesis in portuguese, Centro Federal de Educação Tecnológica Celso Suckow da Fonseca - CEFET/RJ, Rio de Janeiro, Brazil.

Vignoli, L.L.; Kenedi, P.P., 2019, "Elastoplastic Residual Stress in Composite Beams", MATERIALS TODAY: PROCEEDINGS, Vol. 8, pp. 747-752. https://doi.org/10.1016/j.matpr.2019.02.016.

Zaidan, D.I., Kenedi, P.P. and Mano, A.B.W.G., 2019, "Influence of Residual Stresses in Fatigue Life of Partially Yielded Mechanical Parts", Proceedings of the 25th International Congress of Mechanical Engineering, Uberlândia, Brazil. https://doi.org/10.26678/ABCM.COBEM2019.COB2019-2451.

RESPONSIBILITY NOTICE

The authors are the only parties responsible for the printed material included in this paper.